Available online at www.sciencedirect.com
ScienceDirect
Estuarine, Coastal and Shelf Science 77 (2008) 230–244
ESTUARINE COASTAL AND SHELF SCIENCE
www.elsevier.com/locate/ecss

Chronology of the sedimentary processes during the postglacial sea level rise in two estuaries of the Algarve coast, Southern Portugal

T. Boski [a,*], S. Camacho [a], D. Moura [a], W. Fletcher [b], A. Wilamowski [c], C. Veiga-Pires [a], V. Correia [a], C. Loureiro [a], P. Santana [a]

[a] *CIMA – Centro de Investigação Marinha e Ambiental, Universidade do Algarve, Campus de Gambelas, 8000 Faro, Portugal*
[b] *UMR 5805 EPOC – CNRS, Département de Géologie et Océanographie Université Bordeaux 1, 33405 Talence Cedex, France*
[c] *Institute of Geological Sciences, Polish Academy of Sciences, Twarda 51/55, 00-818 Warszawa, Poland*

Received 28 June 2006; accepted 17 September 2007
Available online 16 October 2007

Abstract

Four profiles of estuarine sediments obtained from boreholes drilled in the Algarve, Southern Portugal were studied in order to reconstruct the process of sediment accumulation driven by the postglacial sea level rise. In addition to the sedimentological analysis, the Foraminifera Index of Marine Influence (FIMI) permitted assessment of the nature and organization of sedimentary facies in the Beliche–Guadiana and Gilão–Almargem estuaries. The Beliche–Guadiana CM5 and Almargem G2 profiles accumulated in a sheltered environment, with the former presenting an almost continuous record of the sea level rise since ca 13 000 cal yr BP. The G1 and G3 profiles from the Gilão–Almargem area represent a more discontinuous record of the last 8000 years, which accumulated in the more dynamic environment of an outer estuary. The integration of all radiocarbon ages of dated levels, led to an estimate of sediment accumulation rates. Assuming a constant position of the sediment surface with respect to the tidal range and a negligible compaction of sediment, the sea level rose at the rate of 7 mm yr^{-1} in the period from 13 000 to 7500 cal yr BP. This process slowed down to ca 0.9 mm yr^{-1} from 7500 cal yr BP until the present. The marked historical change in the rate of sediment accumulation in these estuaries also occurred with the accumulation of organic matter and is, therefore, important data for global biogeochemical models of carbon. The main obstacle to obtain higher temporal resolution of the sedimentary processes was the intense anaerobic respiration of organic matter via sulphate reduction, which did not allow any accumulation of peat and, furthermore, led to erasure of the palaeontological record by acid formed from the subsequent oxidation of sulphides.

Keywords: sea level rise; sedimentary record; estuary; foraminifera; Gulf of Cadiz; carbon cycle; climate change

1. Introduction

Estuaries, in common with other geomorphological features on the mobile ocean–continent interface, are subject to rapid changes imparted by either accretion or erosion of sediments. These two concurrent processes are modulated by a series of factors which may be mutually reinforcing or eliminating. Over the period of the last 15 000 years, i.e. the last postglacial period, the most important factors controlling the process of infilling of river paleovalleys in non-glaciated terrains are: eustatic sea level rise, continental erosion, availability of sediment on the shelf, and local hydrodynamics. A comprehensive analysis of the regional sedimentation patterns observed in the estuaries from the Spanish side of the Gulf of Cadiz, has been recently put forward by Lario et al. (2002). Two contrasting physiographic situations may be identified on the Gulf of Cadiz coast, allowing an investigation of the complementary aspects of coastal and estuarine development:

(1) provided that they are located on deeply incised bedrock, sheltered, low-energy coastal embayments may provide

* Corresponding author.
E-mail address: tboski@ualg.pt (T. Boski).

0272-7714/$ - see front matter © 2007 Elsevier Ltd. All rights reserved.
doi:10.1016/j.ecss.2007.09.012

a reliable record of local sea level rise occurring since the Last Glacial Maximum. Such sedimentary environments are protected from episodic high-energy erosion or accumulation events, and thus may retain a continuous record of global/regional climatic and environmental indicators such as Relative Sea Level (RSL), vegetation cover, and connectivity with the open ocean;

(2) in contrast with the above, sites which are more exposed to high-energy processes may better preserve sedimentary indicators of sporadic local events such as marine storms, river floods or tidal currents (Darlymple et al., 1992). In such situations, the coarser grain size of siliciclastic material permits inferences to be drawn about the origin and availability of these sediments.

Within the framework of a long term programme embracing the study of sea level and climatic changes along the South Iberian coast, a series of cored boreholes have been drilled through the sediment infills of the Algarve estuaries (Fig. 1), with the ultimate objective of assessing the quantitative volume of accumulated sediments and their organic matter. This approach should permit coupling the accumulation of postglacial organic carbon in coastal zones with the oscillations of atmospheric carbon dioxide (CO_2) documented during the last 400 000 years. In the present paper, the results are reported for benthic foraminifera, sedimentological and geochemical investigation of two cores (coded CM5 from the Beliche–Guadiana Estuary and G2 from Almargem Estuary) which represent the sheltered situation (1), and two cores (coded G1 and G3) from the Gilão–Almargem Estuary which represent the exposed situation (2). The organic markers of CM5 core have been recently discussed by Gonzalez Vila et al. (2003). The comparison of sediment accumulation which took place during the terminal Pleistocene to Holocene in these two contrasting physiographic contexts will provide insight into the recent geological history of the Eastern Algarve coastline, and will demonstrate the distinction between global and local forcing factors in the sedimentation histories. A similar approach has been taken recently by Bao et al. (1999) for analysis of the Holocene evolution of the Albufeira Lagoon on the Western Portuguese coast, south of Lisbon.

2. The study area

The Algarve coastline is located at the passive continental margin of South West Iberian Peninsula. In geomorphological terms, the Eastern coastal sector where both the estuarine sites are located is dominated by the Ria Formosa Barrier Islands System enclosing a lagoonal body along ca 50 km. The wave regime is predominantly from south west, associated mainly with swell from the Atlantic Ocean. The strong longshore current is west-to-east and the mean tidal range is 2 m, i.e. mesotidal. The Gilão–Almargem Estuary represents the terminal segment of two small river basins totalling ca 290 km^2 and draining a predominantly Mesozoic carbonate and Miocene siliciclastic substratum (Fig. 1). The average precipitation in this zone for the last 75 years is 530 mm yr^{-1} and is concentrated between October and April. At present, the estuarine zone is sheltered behind the Cabanas Island from the Ria Formosa Barrier Island system that was initiated in the early Holocene (Andrade et al., 2004).

At the second site, 20 km eastward, the Beliche River drains a basin of about 125 km^2, which is placed exclusively on Carboniferous shales and greywackes. It is the last significant tributary of the Guadiana, which is the fourth principal river of Iberia in terms of catchment area (67 000 km^2) and length (810 km). The hydrologic regime of Guadiana is characterized by irregular discharges, varying between virtually nil during summer periods and up to a reported 11 000 m^3 s^{-1} for the winter peak of 1876 (Rocha and Correia, 1994), i.e. half a century before the installation of river dams. The Beliche–Guadiana confluence lies within the reaches of the present estuary of the Guadiana. The latter is in the terminal stage of sediment infilling of the paleovalley which was incised down to 80 m depth during the glacial lowstands. The extensive salt marshes, which are developed on the accreted sediments on both sides of the infilled estuary, are covered by halophytic plants: *Spartina densiflora*, *Spartina marítima*, *Atriplex* spp. and *Salicornia patula*. The fluvial sediments, which are exported from the estuary, mix in the proximity of the river mouth with the sediments transported by the longshore current to form the submerged delta (Gonzalez et al., 2004). Tidal currents carry this material back into the system of gullies and channels, contributing to their progressive shoaling. In order to preserve wetland habitats, water circulation is enhanced in these channels through occasional dredging.

3. Methods

The four drilling sites were within the upper reaches of the intertidal zone and were carried out with a WIRTH Bo drilling rig using bentonite slurry and steel casing in order to avoid the collapse of the borehole walls. In all four cases, the borehole mouth was assumed to have elevation of 0 m above the mean sea level. The core barrel was equipped with plastic 6″ coreline™ (Rocbore Ltd.) tube which optimized the recovery of sediment to an average of 80% on a volume basis.

The cores were further sectioned in two halves, one for immediate sampling and the other for archiving. The standard description of the cores included granulometry and macroscopic sedimentary structures. The colour was described according to the Munsell chart in a sequence: hue, value and chroma. Mollusc shells and plant remains were selected manually for dating, during the core analysis. Organic samples were kept at −20 °C and freeze dried before being sent to the commercial laboratories referred to in Table 1 for dating. All the ^{14}C age data are expressed as calibrated years Before Present (cal yr BP).

The samples for organic matter analyses, reported by Gonzalez Vila et al. (2003), and samples for pollen studies, reported by Fletcher et al. (2007) were taken always from the central part of the cores in order to avoid contamination. Pollen and spores, which represent an important source of refractory organic matter, originate from plants growing near the core site and in the

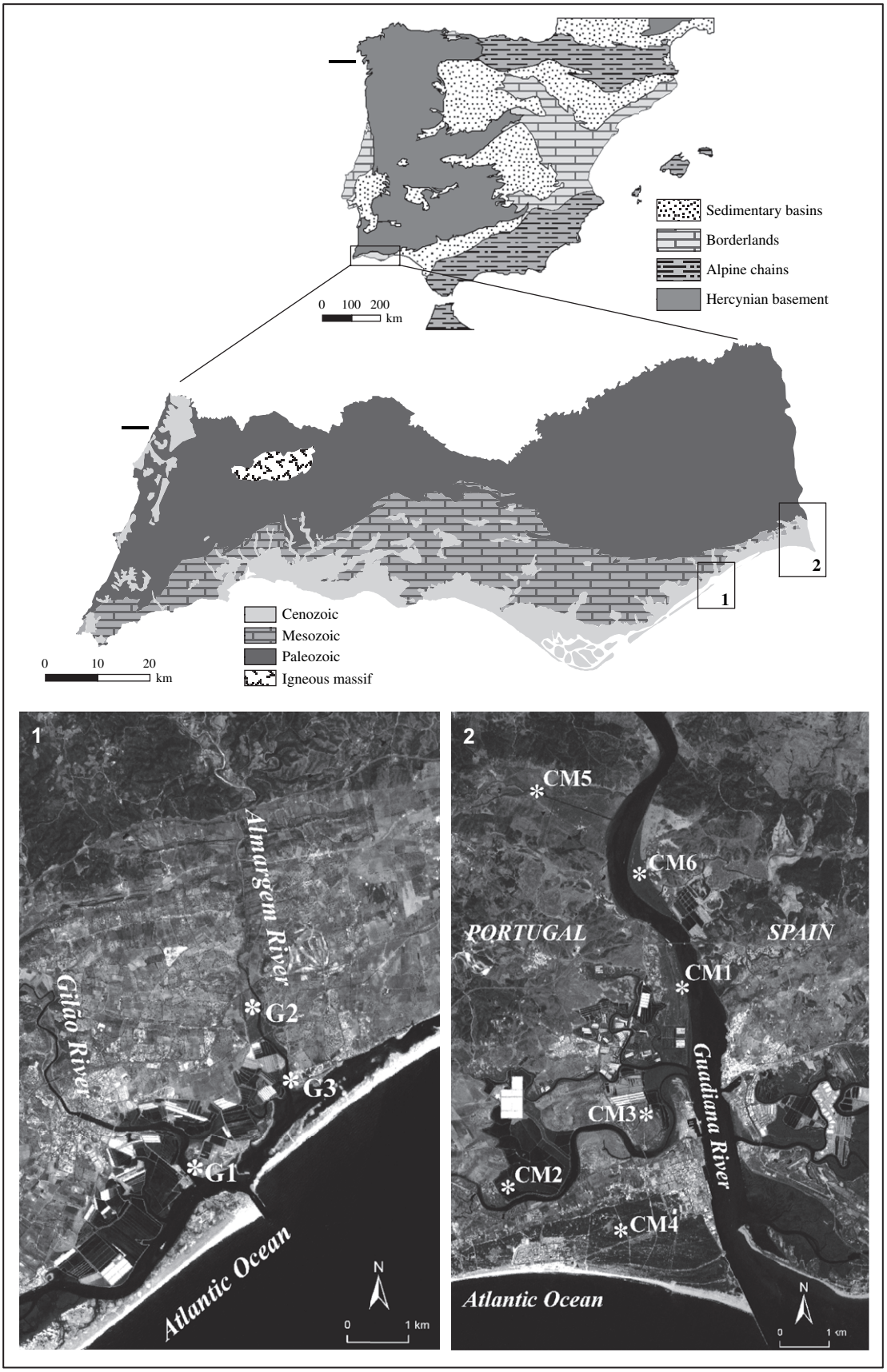

Fig. 1. Indian Remote Sensing Satellite (IRS) panchromatic image showing the localization of the boreholes and geological context of the study area (inset). (1) Boreholes *G1, *G2, *G3 on the Gilão–Almargem Estuary; (2) boreholes *CM1, *CM2, *CM3, *CM4, *CM5, *CM6 on the Beliche–Guadiana Estuary.

Table 1
Summary information on ^{14}C datings. Laboratory codes: β – Beta Analytical, USA; IRPA – Institut Royal du Patrimoine Artistique, Belgium; WK – University of Waikato, New Zealand. Method: Rad. – β radiometric counting; AMS – accelerator mass spectrometry

Borehole/sample depth (m)	Lab. code	^{14}C age (yr)	$\delta^{13}C‰$ PDB	Cal BP (yr)	Material	Method
Beliche marsh						
CM5						
3.33[a]	WK-16012	3375 ± 39	0.2	3220	*Scrobicularia plana*	AMS
5.79[b]	IRPA-15211	4295 ± 35	na	4408	*Venerupis*	AMS
8.90[a]	WK-16013	6764 ± 45		7600	*Cerastoderma glaucum*	AMS
13.45	IRPA-15212	7585 ± 35	na	8017	*Venerupis*	AMS
17.75[b]	IRPA-15210	7725 ± 45	na	8169	*Cardium*	AMS
20.95[a]	WK-16014	8256 ± 55	25.3	9310	Wood	AMS
42.70[a]	WK-16015	10 273 ± 66	25.5	11 448	Wood	AMS
47.67[b]	β-137110	10 990 ± 40	−25.7	12 991	Wood	AMS
Gilão–Almargem Estuary						
G1						
2.03	β-137111	750 ± 40	−24.3	697	Org. matter	AMS
5.79	β-137113	1060 ± 60	0	1035	*Venus*	Rad.
7.45	β-137114	3500 ± 100	0	3890	*Cardium*	Rad.
8.55	β-137117	7130 ± 40	−0.4	7998	*Cardium*	AMS
G2						
2.18	β-137115	2310 ± 40	−23.4	2342	Org. matter	AMS
3.88	β-137116	2300 ± 40	−24.8	2330	Org. matter	AMS
5.30	IRPA-13228	2705 ± 30	−0.14	2439	*Venerupis*	AMS
7.42	IRPA-13227	3380 ± 25	−1.02	3238	*Scrobicularia plana*	AMS
11.35	β-137118	7280 ± 40	−0.9	8113	*Cardium*	AMS
G3						
2.70	β-137119	280 ± 50	+0.2	358	*Cardium*	AMS
3.92	β-137120	1810 ± 90	0	1807	*Cardium*	Rad.
5.92	β-137121	2910 ± 120	0	3150	*Bivalves*	AMS

[a] Data from Fletcher et al. (2007).
[b] Data from Gonzalez Vila et al. (2003).

surrounding region. Besides the contribution of terrestrial taxa from forest, shrub and open ground habitats, almost the entire profile contained abundant pollen and spores from estuarine marsh vegetation.

Grain size analyses were carried out after carbonate elimination with 10% hydrochloric acid (HCl). The samples were sieved through a 250 μm sieve and the fractions <250 μm were analysed in a Malvern Mastersizer Microplus instrument using demineralized water with 1 g of Calgon l^{-1}, added to avoid flocculation of clay minerals. The results of granulometric analyses are presented together with lithological profiles, in the form of mean grain size plots.

The mineral composition of selected sandy samples was identified by transmission light microscopy, electron microprobe and X-ray diffraction (XRD) of powder in capillary tubes. Samples were separated into density fractions using bromoform. The heavy fraction yields were close to 1 wt%. Density fractions were used to prepare polished thin sections of grains submerged in Araldite resin. Additional magnetic separation of the heavy fraction was carried out to concentrate siderite for better XRD powder patterns. Chemical identification was carried out by the microprobe "JEOL 840A" equipped with a "Noran" energy-dispersive detector using an accelerating voltage of 15 kV. Clay mineralogy was determined, semi-quantitatively in orientated aggregates, by XRD using a Philips PW 1390 apparatus, and Cu Kα radiation (30 kV, 30 mA). Diffractometric analyses comprised three treatments for the samples: (1) air dried; (2) solvated with ethylene glycol vapours; and (3) heated to 500 °C. The nomenclature of clay mineral species followed that proposed by Thorez (1976).

The samples for benthic foraminiferan analyses were sieved through 500 and 63 μm sieves after decanting away the organic debris. After sieving, samples with a high sand content were dried and the sediment was sprinkled into carbon tetrachloride to float off the foraminifera. Samples with high total numbers of foraminifera were divided with a modified plankton splitter (Scott and Hermelin, 1993), which divided the sample into eight equal parts in order to reduce the total number of individuals to an optimal 300–400, that were a statistically significant base for characterising each foraminiferan assemblage. However, due to the frequent scarcity of identifiable foraminifera in the cores from the Algarve, 100 were considered to be an adequate number of individuals, supported by the study of Fatela and Taborda (2002). The processed samples were examined under a binocular microscope in a gridded circular counting tray.

From the abundance data, the following parameters were calculated: Shannon diversity index (H'), species dominance and constancy, and agglutinated/calcareous foraminiferan ratio. Q mode cluster analysis was performed on the double root-transformed data matrix, from which species were eliminated

with constancy lower than 50% and abundance below 5%. The double root-transformation technique was applied in order to attenuate the relative importance of very abundant species and increase the weight of rarer ones, before computing the Bray–Curtis similarity coefficient (Field et al., 1982). Grouping of the samples by Q mode cluster analysis permitted the introduction of a new five degree Foraminifera Index of Marine Influence (FIMI) described by Camacho (2006).

4. Results and interpretation

4.1. Interpretation of core CM5 Beliche–Guadiana

4.1.1. Lithology and foraminifera fauna, CM5 borehole

The complete lithological section with radiocarbon ages is presented in Fig. 2. The integrated characterization of foraminifera assemblages within the sedimentary sequence is summarized in terms of Shannon diversity index H' and of Foraminifera Index of Marine Influence (FIMI) in Fig. 3. The complete list of species, which have been identified and included in the statistical grouping is shown in Table 2.

4.1.1.1. Unit I (50.3–48.6 m). The contact between the Carboniferous shale substratum and the directly overlying gravel (Unit I) has been detected at a depth of 50.8 m. The gravel layer is composed of shale, greywacke and quartz pebbles, moderately to well rounded, from 10 to 80 mm in size. Towards the top of the Unit I, there is a 1.7 m layer of medium to coarse sand, of ochre tint (Munsell colour 2.5Y 4/3), containing abundant mica and sparse shale and quartz pebbles. Both layers are remnants of a fluvial regime prevailing during the past lowstands.

4.1.1.2. Unit II (48.6–40.8 m). The initial 3 m layer is silty, with several intercalations of fine hydromica, containing sand of 200–300 mm thickness. The clay fraction comprises in decreasing order: illite, interstratified 10–14c, interstratified 10–14v; and kaolinite, interstratified 10–14sm (Table 3). Organic matter, besides the finely disseminated humic material which was investigated by Gonzalez Vila et al. (2003), is present also in the form of either charred debris or centimetric laminae, enriched with remnants of macerated vegetation.

There are five sandy layers from 45.8 to 40.8 m depth, which contain hydromuscovite, frequent flaser and bioturbation structures. The regular interlaminations of compact silt indicate an intertidal environment similar to the observations by Choi and Park (2000) and Hori et al. (2001) from the Yellow Sea off China.

The initial foraminifera, namely *Trochammina inflata*, *Trochammina* sp., and the internal linings occur at 44.9 m, in the horizon where the regular sand/silt intercalations are attributed to tidal sedimentation. The confined brackish conditions of the salt marsh remain rather constant to the depth of 35.3 m; these conditions enable only the accumulation of a limited number of species, where the acid conditions hamper the preservation of foraminiferan tests in significant quantities. The FIMI of this segment varies between (1) without foraminifera; and (2) in which *Trochammina* genus dominates, accompanied by the inner linings.

4.1.1.3. Diagenetic minerals in the heavy mineral fraction from Unit II. According to Rey et al. (2005), magnetic susceptibility may reveal diagenetic remobilization/enrichment of sediments in redox sensitive metallic elements like iron (Fe) or manganese (Mn). Therefore, the mineralogical composition of two, fine sand samples taken at 47.30 and 40.9 m depth, i.e. within the high susceptibility area (Fig. 2) has been examined in detail. The composition of both samples is quite homogenous with regard to the dominant quartz and feldspar grains, accompanied by ca 10% shale lithoclasts of moderate to poor roundness. The composition of the residual sediment, after subtraction of the low density fraction, is more variable both in the kind of minerals and in their relative abundance. The main mineral components of the heavy fraction are tourmalines, amphiboles, pyroxenes, garnets, staurolite, andalusite, and Fe-oxides and carbonates. On both samples, siderite-like carbonate grains are round in shape, often showing the presence of cracks. In back-scatter electron images, the cracks appear to be the effect of the deep relief in the grain's surface, with the voids usually filled by fine sediment particles. Electron microprobe analysis of these grains reveals a variable and complex chemical composition. As a rule, the carbonate grains have a thin outer rim which is more calcic (Ca) than the inner parts which are richer in Fe and magnesium (Mg). The scanning electron microscope (SEM) image exhibits a clear zonation which corresponds also to the changes in proportions between the Fe, Ca, Mg and Mn carbonate system (Fig. 4).

The formation of these complex phases occurs as a result of the oxidation of pyrite, distributed within the sediment and exposed to circulating groundwater. A subsequent precipitation of siderite is accompanied either by incorporation of other metals into its crystal lattice or by the precipitation of discrete carbonate phases. The carbonate ion in the interstitial solution may originate from the dissolution of the calcium carbonate, for instance, in the form of foraminiferan tests, or from the dissolution of carbon dioxide (CO_2) produced by bacterial oxidation of the organic matter (Choi et al., 2003), or from methanotrophy postulated by Mata et al. (2005). Similar macroscale zonations of minerals are common in the proximity of acid mine tailings, and have been described by Ptacek and Bowles (1994) and Hossner and Doolittle (2003). Pyrite has not been observed in these samples; although it has been frequently identified along the upper portion of the CM5 profile during the micropaleontological work, in finely distributed form, or as the infilling of foraminiferan chambers.

4.1.1.4. Unit III (40.8–24.5 m). From 40.75 to 37.75 m, the sediment is composed of fine compact silt, dark grey in colour (2.5Y 2.5/1) and containing centimetric layers enriched with macerated plant remains. These accumulations of organic matter (OM) indicate an intertidal environment of deposition and are equivalent to the intercalations of peat in a wetter

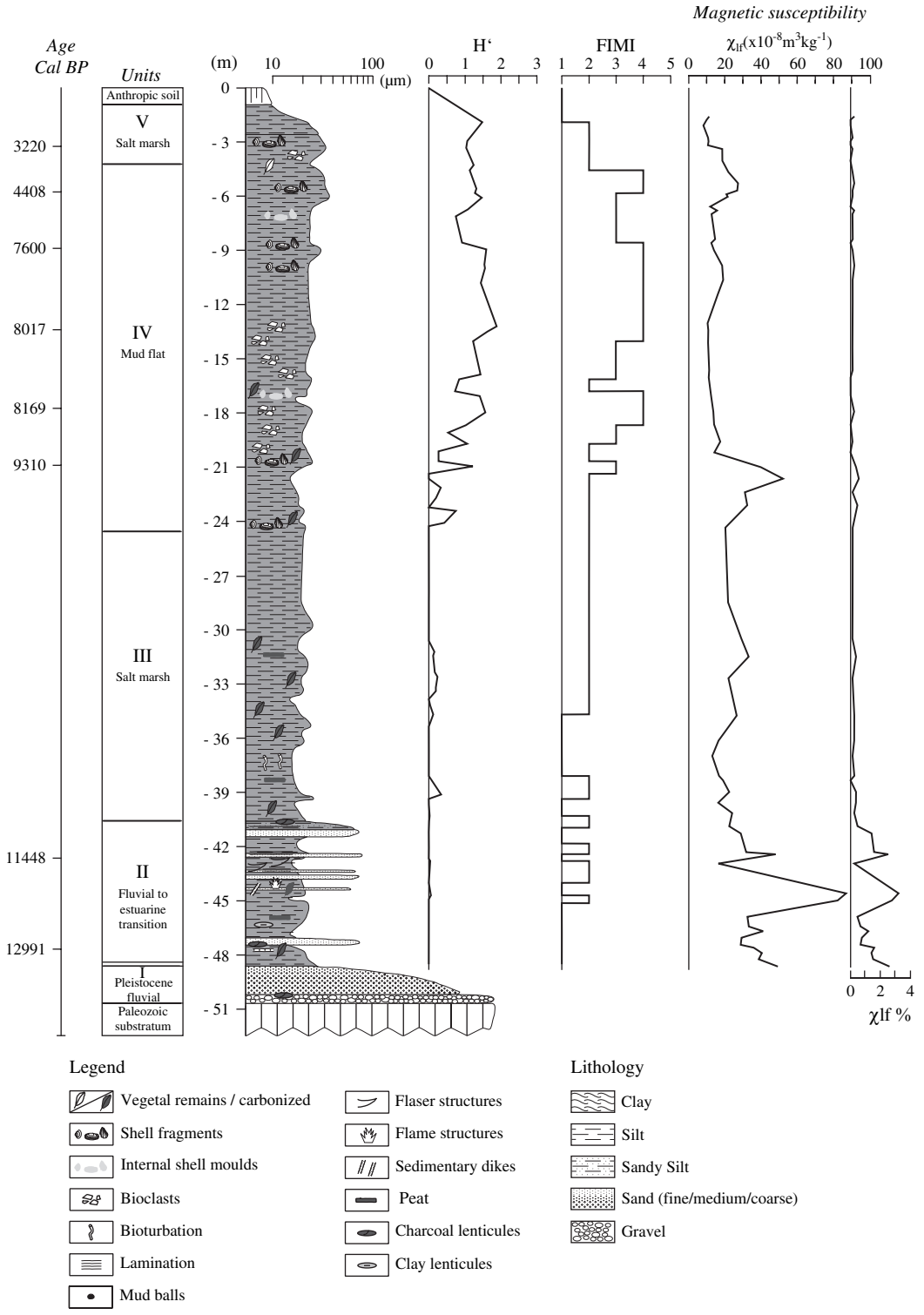

Fig. 2. Lithological profile of borehole CM5 in Beliche–Guadiana Estuary, with graphs showing the magnetic susceptibility, the variation of Foraminifera Index of Marine Influence (FIMI) and Shannon diversity index of foraminifera.

climate and to depositions at wider ocean–continent interfaces such as the NW Europe coast. Hence, according to Allen (2000), such layers can be considered as reliable indicators of Relative Mean Sea Level (RMSL). Towards the top of the sequence, these OM layers become sparse, the last being observed at 31.2 m depth. Most probably, the local environment changes from the upper (salt marsh) to the lower (mud flat) intertidal level, with little or no halophyte vegetation covering the sediment surface. The limit between these two lithofacies is placed at 24.5 m depth, i.e. where the first appearance of macrofauna has been observed. The shells, which are frequently corroded by dissolution, belong mostly to the bivalve genera: *Spisula*,

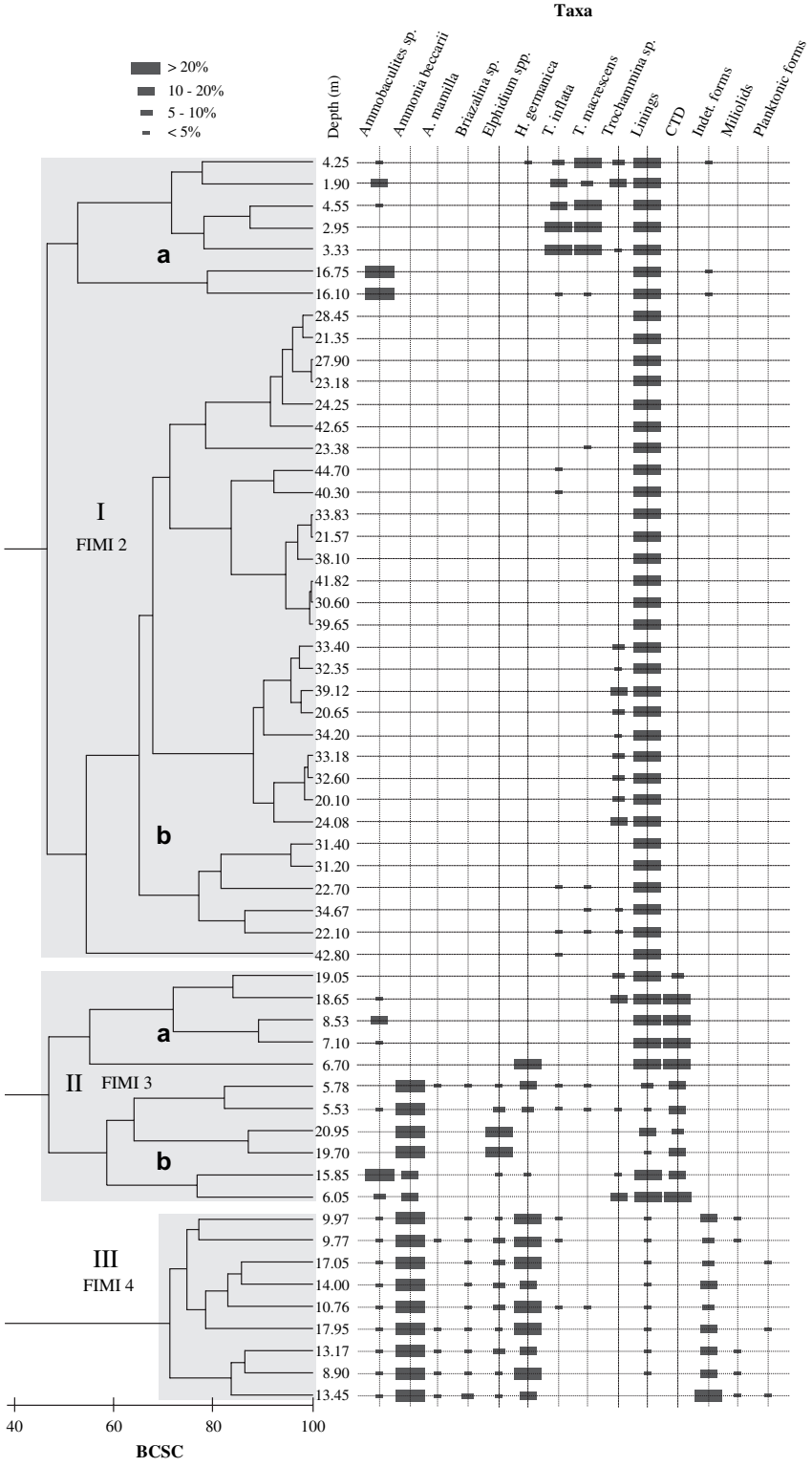

Fig. 3. Cluster analysis of foraminifera assemblages in the borehole CM5 and the resulting classification (right) of analysed samples along the entire profile. The curve shows the variation in the number of the foraminifera species. Abundance of species: >20% dominant; 10–20% common species; 5–10% accessory species; <5% rare species. BCSC – Bray–Curtis similarity coefficient; CTD – carbonate tests showing dissolution.

Scrobiculária, *Acanthocardia*, *Cerastoderma*; and gastropod genera: *Nassarius*, *Tomus*.

In terms of foraminiferan content, the entire Unit IV continues with a predominance of inner linings and an occasional *Trochammina* spp. The diversity values are low, oscillating around $0.1H'$, with an invariable FIMI value of 2. The stable conditions of the middle to upper salt marsh prevail for a period of ca 3000 years (Fig. 6). At 20.95 m depth, the FIMI rises to

Table 2
List of foraminifera species determined in borehole samples from two estuaries

Agglutinated species	Calcareous hyaline species	Other groups
Ammobaculites sp.	*Ammonia beccarii* (Linné, 1758)	Linings – inner linings
Trochammina inflata (Montagu, 1808)	*Brizalina* sp.	CTD – carbonated tests in dissolution
Trochammina macrescens (Brady, 1870)	*Elphidium advenum* (Cushman) var. *margaritaceum* (Cushman, 1930)	Planktonic forms – all planktonic forms
Trochammina sp.	*Elphidium* spp.	Miliolids – all porcellaneous species
	Elphidium advenum (Cushman, 1922)	Indeterminate – very small and damage tests
	Elphidium advenum (Cushman) var. *margaritaceum* (Cushman, 1930)	
	Elphidium complanatum (d'Orbigny, 1839)	
	Elphidium crispum (Linné, 1758)	
	Elphidium excavatum (Terquem, 1876)	
	Elphidium gunteri (Cole, 1931)	
	Elphidium gunteri (Cole) var. *galvestonensis* (Kornfeld, 1931)	
	Elphidium macellum (Fichtel & Moll, 1798) var. *aculeatum* (Silvestri, 1900)	
	Elphidium poeyanum (d'Orbigny, 1839)	
	Elphidium sp.	
	Elphidium williamsoni (Haynes, 1973)	
	Asterigerinata mamilla (Williamson, 1858)	
	Haynesina germanica (Ehrenberg, 1840)	

the value of 3 showing a dominance of the agglutinated forms *Trochammina inflata*, *Trochammina macrescens* and *Ammobaculites* spp., accompanied by the unidentified corroded carbonate tests. FIMI 3 suggests a mid-tidal environment where exposure to subaerial conditions is sufficiently long to promote the dissolution of calcareous tests.

4.1.1.5. Unit IV (24.5–4.2 m). Above 24.5 m, sediment mean grain size is restricted to a narrow range between 15 and 30 μm, and has a regular dark colour (2.5Y 2.5/1); however, the two levels 16.9–15.80 m and 13.4–13.2 m are exceptional with a much lighter and patchy appearance and kaolinite content over 20% (Table 2). The increase in the quantity of kaolinite is attributed to the acidification of sediment through the diagenetic oxidation and dissolution of pyrite, similar to the observations on Cretaceous mudstones by Pe-Piper et al. (2005). The rise of magnetic susceptibility in the interval 23–21 m is once more attributed to diagenetic Fe minerals. In the uppermost part of the profile, millimetric idiomorphic crystals of gypsum have been observed under the microscope in the samples from 6.10, 6.05 and 4.25 m.

Up to the depth of 5.53 m, the foraminiferan assemblage in Unit IV is highly variable. The most common FIMI value in this depth interval is 4, characterized by the co-dominance

Table 3
Semi-quantitative estimation of principal clay mineral species in the silty samples from borehole CM5. 10–14c, 10–14v and 10–14sm are interstratified clay species: illite–chlorite, illite–vermiculite and illite–smectite, respectively

Depth	Illite	10–14c	10–14v	Kaolinite	10–14sm
333	63	15.7	9.8	8.7	2.8
533	56	18	9.2	13.6	3.2
890	56.5	12.4	8	11.3	11.8
997	62.7	8.1	11	12.9	5.2
1317	49.7	15.4	8.4	20.9	5.6
1675	57.1	12.4	6.9	20.7	2.9
2090	54.5	22.4	12.1	7.9	3.1
2318	55	17.7	5.3	16	6
2425	53.6	19.8	7.9	14.3	4.4
2845	64	5.2	9.8	13.1	4.9
3060	56	17.4	7.7	14	5
3260	57	17.6	6.8	15.2	3.4
3467	64.9	9.5	11.4	11.5	2.7
3710	57.4	13.3	13.5	10.8	5
3965	61.6	13.9	7.9	13.9	2.8
4120	72	9.2	10.8	7	1
4490	54.4	17	10.3	16	2.4
4833	54.7	17.2	15.6	9.4	3.1

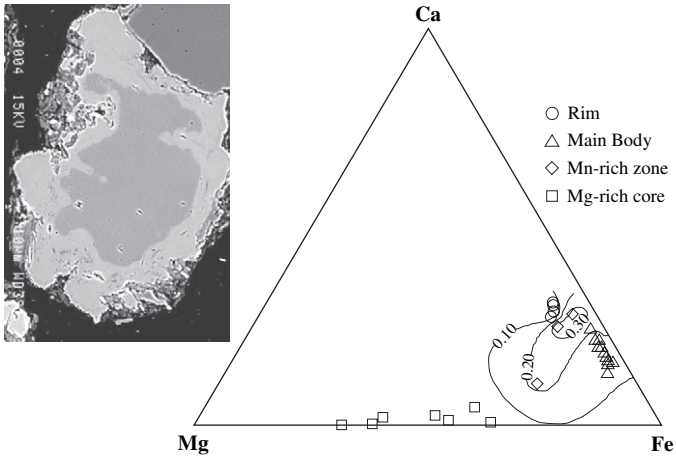

Fig. 4. Back-scatter electron image (left) of the siderite concretion. The boundary of the core (dark) composed of Fe and Mg carbonate resembles the grain shape and is enriched in Mn. Semi-ternary diagram (right) in a four-component system showing the chemical compositions in mol% of four different compositional zones in siderite concretions presented in the image. For the purpose of the triangle presentation, compositions were normalized to 100 with regard to three variables: Ca, Mg and Fe, and the true Mn-contents were presented as isolines. The actual Ca, Mg and Fe-contents can be read out directly from the triangle after subtraction of Mn-contents.

of *Ammonia beccarii* and *Haynesina germanica*, associated with *Elphidium* spp. The abundance of the two former species is never lower than 60% which, according to Edwards and Horton (2000), is typical for estuarine conditions where only occasional subaerial exposure is experienced. The frequent *Brizalina* spp. is considered to be an exotic species, brought into the estuary from the continental shelf by hydrodynamic processes (Mendes et al., 2003).

4.1.1.6. Unit V (4.2–0 m). From 4.2 m to the surface, the traces of halophyte rootlets and other vegetal remains reappear in the sediment. The top 2.4 m of the sediment column, with colour (10YR 5/1), displays a patchy appearance due to exposure to oxidizing conditions, possibly related to the agricultural activity which is known in this area since the fifth century BC (Berrocal-Rangel, 2001). This upper interval preserves the foraminifera fauna of a strongly confined environment with associated FIMI value 2, where the inner lining group of *Trochammina macrescens* and *Trochammina inflata* is dominant. *Ammobaculites* sp. and *Trochammina* sp. occur as secondary species.

4.1.2. Reconstruction of environmental changes during the process of infilling in Beliche area of Guadiana Estuary

There is no datable organic matter nor skeletal remains within the 2.2 m thick, gravel/coarse sand of Unit I (Fig. 2), lying directly on the Palaeozoic substratum; although the equivalent layer in the Spanish estuaries of the Gulf of Cadiz has been ascribed by Dabrio et al. (2000) to the Marine Isotopic Stage (MIS) 3. The chronologically resolved sedimentary record in borehole CM5 begins with a silty layer in Unit II, containing wood fragments dated 12 991 cal yr BP, at 47.67 m depth; no foraminifera have been observed at this level. However, intertidal foraminifera do occur in Unit II above the 47.67 m level before the second dated level, at 42.70 m, with an age of 11 448 cal yr BP. Therefore Unit II, which in stratigraphical terms corresponds to the Younger Dryas (YD) stadial (Gulliksen et al., 1998), may be attributed to a transitional fluvial/marine origin. Given the lack of any observable discontinuity in lithology, it may be assumed that this transition occurs within the Guadiana Estuary without any major interruption in sedimentation. Indeed, at a similar depth of 45 m in the Ria de Vigo, Galicia, Spain, seismic reflection profiles also show a clear discontinuity which can be attributed to the YD stadial (García-García et al., 2005). Moreover, in the borehole CM5 on the Guadiana Estuary, the depth–age relation for the period between 12 991 and 7600 cal yr BP, comprising six dated points (Table 1), fits a linear regression trend of 0.73 m per century with a squared correlation coefficient $R^2 = 0.971$. This correlation points to a remarkably constant sediment accretion rate and, consequently, there is no evidence supporting the regional sea level drop during the YD, postulated by Rodrígues et al. (1991). Due to the good hydraulic conductivity, the sand/silt interlaminations within the Unit II enhance the ground water circulation, which provides the oxidizing conditions for the dissolution of pyrite, that may explain the presence of secondary Fe–Mg–Mn–Ca carbonates described in Section 4.1.1.

Unit III, which extends to the depth of 24.5 m, provides no datable organic or shell material. Marsh vegetation which is dominant in the pollen record of this interval (Fletcher et al., 2007) may exclude bivalve shells that are more characteristic of channel margins and unvegetated flats (Borrego et al., 1995). In addition, the intensity of anaerobic respiration related to sulphate reduction may prevent the in situ preservation of significant organic material and, indirectly through pyrite formation, allow acidification of sediment which would dissolve skeletal carbonates of shells. Nevertheless, the conspicuous continuity of FIMI value of 2 throughout most of the interval indicates that Unit III has been an intertidal salt marsh environment.

The local change of the sedimentary facies from the upper (salt marsh) to the lower (mud flat) intertidal level, with little or no halophyte vegetation covering the sediment surface, is marked by the first appearance of macrofauna. The limit between these two lithofacies (Units III and IV) is placed therefore at 24.5 m depth, i.e. the first appearance of bivalve *Scrobicularia plana*. From this level upwards, the continuous presence of macro and microfossils, combined with scarcity or absence of plant root traces and other vegetal remains, indicates that the sedimentary Unit IV (24.5–4.2 m) had been deposited as a non-vegetated or scarcely vegetated mud flats bordering the Beliche channel.

The appearance of gypsum in the topmost segment of Unit IV is a clear signal for the terminal stage of sediment infilling within the estuary. At this stage, conditions are favourable for the formation of small water ponds, which could be replenished during the spring tides and subsequently subject to desiccation. The lack of any discrete layer containing evaporitic minerals suggests that their precipitation occurs in the desiccation cracks rather than directly from solution, as reported by Morhange et al. (2000).

The uppermost Unit V has much less macrofauna preserved than the underlying Unit IV. Microfauna indicates a confined environment in the final stage of infilling of the estuary, with the halophyte salt marsh vegetation covering the sediment surface.

4.2. Interpretation of G cores, Gilão–Almargem Estuary

The lithological profiles of three boreholes with ^{14}C dating information and granulometry are presented in Fig. 5. Thirty-three samples from three boreholes have been analysed for their benthic foraminiferan content, of which only 23 give quantitatively significant results. For this reason the Q mode grouping has not been done, and instead the criteria for the attribution of FIMI have been applied through analogy with borehole CM5. FIMI values are plotted together with the lithological profiles (Fig. 5), except for borehole G3 in which only one sample contains microfauna.

4.2.1. Lithology and foraminiferan fauna: G1 borehole (Gilão area)

The total length of this core is 17.7 m with a total of 15 samples analysed for their microfauna content. The sedimentary

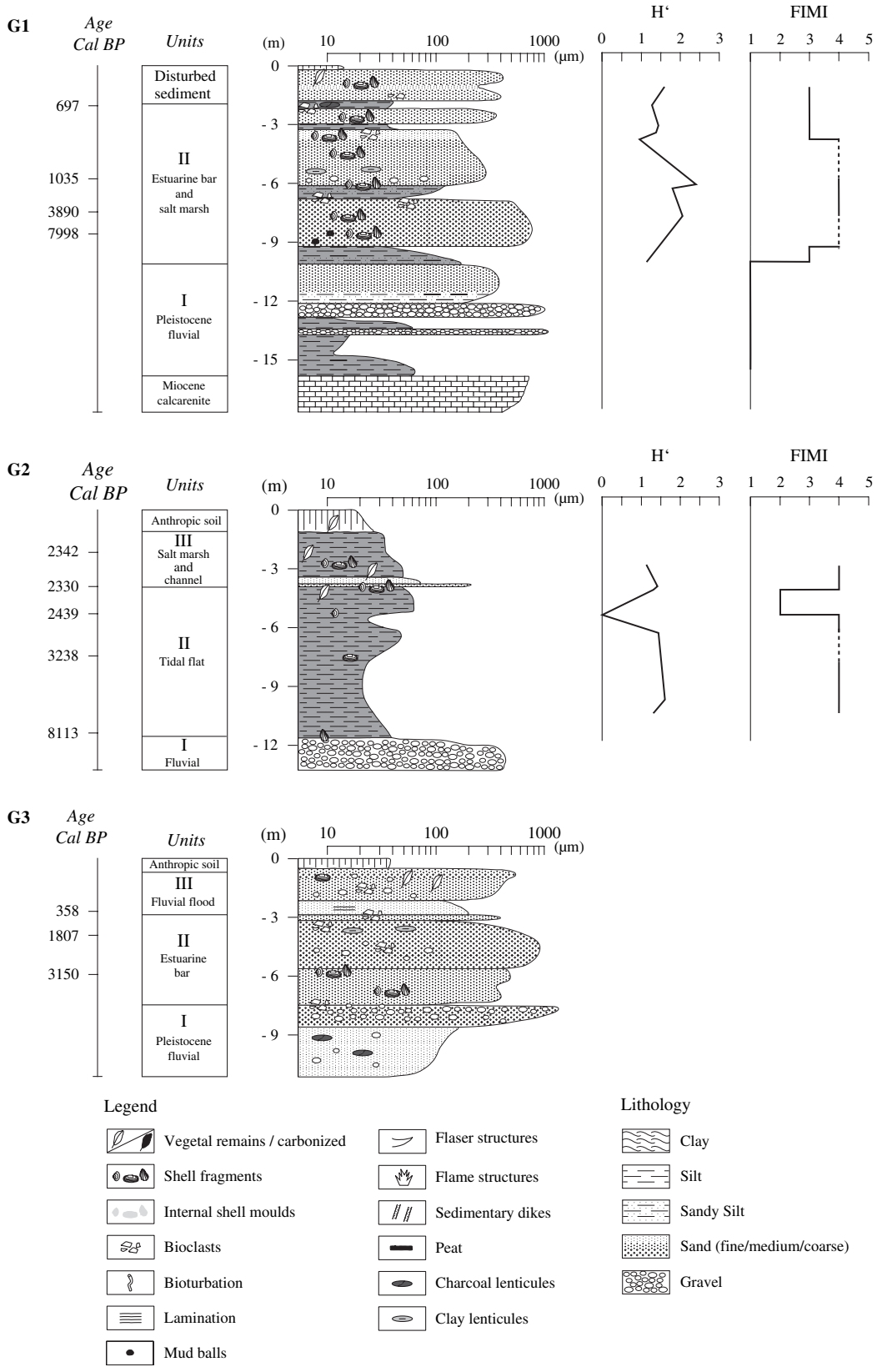

Fig. 5. Lithological profiles of boreholes G1, G2 and G3, Gilão–Almargem Estuary with graphs showing, the variation of Foraminifera Index of Marine Influence (FIMI) and Shannon diversity index of foraminifera. Dotted line indicates the inferred FIMI value, for the levels in which the foraminifera tests were diagenetically dissolved.

segment between 17.7 and 15.8 m depth is a light yellow, porous calcarenite belonging to the Tortonian Cacela Formation (Studencka et al., 2003).

4.2.1.1. Unit I (15.8–10.1 m). The Miocene bedrock is overlain by 1.9 m of yellowish-brown (10YR 5/6), clayey silt with a 30 cm layer of well rounded discoidal, 50–100 mm greywacke gravel. The clayey fraction of silt is composed of 73% illite, 19% kaolinite, and a residual content of chlorite and interstratified species. A sharp discontinuity separates the silts from the overlying 0.8 m bed of gravel which is composed of poorly rounded, 20–80 mm, Carboniferous greywacke pebbles transported by the River Gilão from the Palaeozoic outcrops ca 8 km northwards. The gravel/silt interlayerings belong stratigraphically to fluvial Pleistocene formations of Algarve described by Moura and Boski (1999). On top of this coarse sediment, and up to 9.2 m depth, lies an upwards fining sequence, whose lower part (12.1–10.1 m) is a light grey (10YR 7/2) to ochre yellow, partially indurated by carbonate cement and medium to silty sand. Similar textural features of Late Quaternary and Holocene alluvial deposits have been recently described by Nanson et al. (2005). No foraminifera occur in this Unit.

4.2.1.2. Unit II (10.1–1.9 m). Despite the lack of lithological contrast with the former unit, the grey to ochre carbonate, containing hardened silt which yields no macrofauna, has been ascribed to Unit II due to the presence of benthic foraminifera. At 9.2 m, there is a marked discontinuity in the silt with an overlying layer of grey, medium to coarse sand containing abundant bioclasts of molluscan macrofauna. Quartz grains are well rounded, with a heavy mineral content below 1 wt% in three of the analysed samples, containing ilmenite, zircon, rutile and tourmaline. This discontinuity marks the occurrence of highly dynamic conditions prevailing in an estuarine channel open to marine circulation. The sedimentary sequence continues up to 2.9 m depth with alternating sand and sandy silt layers and an abundant bioclastic fraction, which reflects an environment of varying hydrodynamism within an estuarine lagoon. Molluscan shells in various states of preservation are represented by three species: *Tapes decussatus*, *Cardium* sp. and *Ostrea edulis*. The top 2 m is disturbed by human activity and is not interpreted.

At 10 m depth, the analysed sample contains exclusively calcareous taxa, and according to the grouping procedure has been classified as a FIMI value of 3. At 9.2 m depth, in the coarse sandy layer, only a few foraminifera have been preserved, as is also the case for the sample at 5.8 m depth. However, both samples belong to the same sedimentary unit as the samples at 7.7, 6.3 and 6.1 m depth, where the foraminiferan assemblage is almost entirely calcareous. The unequal fossil fauna content is due to taphonomic processes and, therefore, all five samples are considered as belonging to the FIMI 4 group. In the calcareous assemblage of the three later samples, the species *Ammonia beccarii* and *Haynesina germanica* dominate, with cumulative abundances (varying between 33.3 and 59%); these species are associated with *Elphidium* spp. group and the more marine groups: *Asterigerinata mamilla*, *Cibicides lobatulus*, and miliolids. According to Donnici and Serandrei-Barbero (2002), Discorbidae and Cibicidae taxa are typically found on substrates with abundant sand and vegetation and in nutrient-poor environments. The presence of miliolids is indicative, according to Redois and Debenay (1996), of slightly hypersaline, restricted environments which may prevail in a more enclosed part of a lagoon. In the uppermost 4 m, *Ammonia* and *Haynesina* still dominate, although the agglutinated species increase up to 18% of the total, reflecting more confined brackish conditions (Haslett et al., 2001).

4.2.2. Lithology and foraminiferan fauna: G2 borehole (Almargem area)

4.2.2.1. Unit I (13.2–11.7 m). This 13.2 m deep sedimentary sequence starts with a 1.5 m layer of reddish-brown (2.5YR 2.5/3) clay, containing sporadic pebbles of limestone and carbonate concretions. No fauna have been observed in this layer.

4.2.2.2. Unit II (11.7–5.1 m). At the depth of 11.7 m, the sediment changes colour to dark grey (10YR 3/1), reflecting a typical low-energy estuarine environment. The carbonate concretions disappear and the silt contains dispersed remains of decomposed plant material and of corroded bivalve shells, which probably reflect a mud flat environment. In the 7–8 m interval, the sampled material produces a strong sulphur odour and soon after exposure is covered with yellow straw-coloured (2.5YR 8/6) efflorescence of jarosite which is the end product of reaction between the diagenetic sulphuric acid and the sediment (Fitzpatrick et al., 1993). From the total of 11 samples analysed in the borehole G2, the first one containing foraminiferan tests occurs at 10.5 m depth. With the exception of one sample taken from this regular sequence, the foraminiferan assemblage is dominated by *Ammonia beccarii* and *Haynesina germanica* association, with cumulative abundances varying between 13.8 and 79% linked to the group of *Elphidium* spp. The secondary taxa are *Asterigerinata mamilla* and the group of indeterminate forms. The upwards continuity of this assemblage classified as FIMI value 4 is interrupted by the acid horizon (7–8 m). The sample at 5.3 m, where only remnants of agglutinated *Trochammina* tests occur, indicates a vegetated marsh environment and has been attributed to FIMI 2.

4.2.2.3. Unit III (4.8–0 m). The base of this unit is marked by coarse lithoclastic and quartz grains with macerated vegetal detritus. Between 3.8 and 3.4 m depth, the sediment is sandy with abundant shells of venerids and oysters and contains abundant vegetal detritus, reflecting most probably the deposition within a small gully. The FIMI of this interval has a value of 4. The top 3.6 m of the core consists of dark brown (10YR 3/3), silty sediment rich in vegetal remains with root traces at

1.6 m depth. This top section reflects terminal infilling and the growth of halophyte vegetation.

4.2.3. Lithology and foraminifera fauna: G3 core (Almargem area)

4.2.3.1. Unit I (11.2–8.6 m). From 10 to 8.6 m depth, the sediment is a yellowish-brown (10YR 5/4), hard silty sand, rich in carbonate, containing charcoal lenticules and the occasional, poorly rounded pebbles of limestone.

From 8.6 to 7.5 m, the sediment is gravel composed of well rounded, mostly quartz and quartzite pebbles ranging in size from 20 to 70 mm. This Unit does not contain any remnants of fauna and seems to be of fluvial origin, analogous to the gravel/silt interlayers described for borehole G1.

4.2.3.2. Unit II (7.5–2.9 m). The section overlying Unit I is from 7.5 to 2.9 m depth, starting with a 200 mm thick layer of dark grey (2.5Y 3/1) silt, containing remnants of shells and plants. The rest of Unit II is mainly a grey (10YR 7/1), medium sand with up to 7% of a silt/clayey fraction composed by 64–65% of illite and 20–28% of kaolinite; the residual percentage is chlorite with interstratified species. The sediment is rich in vegetal remains with the bioclastic fraction poorly represented or totally absent. From the seven samples initially collected for microfauna analysis, only one at 7.4 m, provides a statistically valid quantity of foraminifera. Carbonate dissolution within the sandy sediment is responsible for the relative rarity of foraminifera. The statistically valid sample has a FIMI value of 4 based on the composition: the *Ammonia beccarii* and *Haynesina germanica* association with a cumulative abundance of 33.7%, *Asterigerinata mamilla* with 22.6%, and *Elphidium* spp. with 12.4%; the indeterminate groups account for 11.1% of the total.

This sequence could represent either a delta fan environment or a submersed estuarine sand bar that has accumulated fine suspended particles of fluvial origin.

4.2.3.3. Unit III (2.9–0 m). This Unit is composed of a 0.5 m layer of a dark grey medium sand, overlain by 2.4 m of coarse, brownish sand mixed with brownish silt (7.5YR 5/2) and containing abundant humified plant detritus. It is also characterized by a high proportion (12%) of lithoclasts, occasional pebbles and some bioclasts on top. At 2.2 m depth, heavy minerals account for 7 wt% of the sample with diagenetic siderite and goethite making up 82% of the total. Magnetite, ilmenite, pyroxene and rutile are the most common minerals in descending order of abundance.

4.2.4. Reconstruction of environmental changes during the process of infilling in the Gilão–Almargem Estuary

In two of the three study sites (G2 and G3), the Holocene estuarine sediments are deposited on top of Pleistocene fluvial sequences lying in shallow paleovalley settings eroded into Upper Miocene bedrock (which was detected only in borehole G1, directly under the Holocene). The first dated signals of marine transgression within this small estuarine system are recorded around 8 k yr BP. In the most inland location (G2), the marine *Cardium* shell from 11.4 m depth dates to 8113 cal yr BP. Due to the sheltered position, the subsequent sedimentation corresponds to a tidal flat setting, interrupted by channel action that has deposited 400 mm of sandy material (Fig. 5). This discontinuity probably explains the recent age of the dated point, which at 2342 cal yr BP (Fig. 6), is clearly above the linear trend of sediment accumulation.

The first appearance of rich and diverse microfauna, within the sandy silt layer of borehole G1, is at 10 m depth within the Unit II. Light hues with reddish patches indicate that this tidal flat sediment has been temporarily exposed to air before being covered by an estuarine bar sand. In this coarse sand horizon, rich in clasts of macrofauna with only a few foraminifera preserved, shells of *Cardium* from 8.5 m depth yield an age of 7998 cal yr BP. According to the works of Pilkey et al. (1989) and Bettencourt (1994), this age roughly corresponds to the beginning of the formation of Ria Formosa barrier island system. Indeed, the process of barrier accretion could only be initiated after the sea level approached the present one, i.e. when the local continental sources of sand such as the sandy cliffs of the Western Algarve (Granja et al., 1984) could supply the eastward longshore current with clastic material. The present annual volume of sand transported eastwards along the Algarve coast and accumulated at the Guadiana Estuary is estimated to be 1.7×10^5 m^3 (Boski et al., 2002). As may be deduced from the sequence of three dated points (at 2, 5.8 and 7.5 m), the bar sediments have been accumulated in several pulses of accretion with sandy material transported through the tidal inlet of the lagoon. FIMI values in these samples range from 4 to 3. The silty intercalations between the sand layers correspond to fine grain drapes described recently by Carling et al. (2006) for the Severn Estuary, UK. Consequently, the entire Unit II may be interpreted as reflecting a land–ocean interface dominated by fluviotidal dynamics that have shaped the outer reaches of the estuary.

The sediment profile of the borehole G3 is limited to only 4.9 m (7.7–2.9 m) of the Holocene deposition which, from the faunal content and lithology, can be classified as estuarine. An exposed position (Fig. 1) and the elevation of the pre-Holocene substratum are responsible for this reduced record

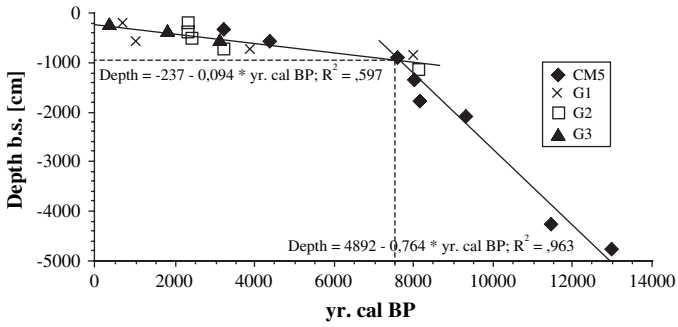

Fig. 6. Depth vs. age graph of the dated sediment levels from Beliche–Guadiana and Gilão–Almargem estuaries. The linear regression equations and the respective plots were computed independently, for lower and upper segments of the profiles, intercepting at 7500 cal yr BP.

which embraces a period of little more than 3000 yr. The clastic material, that forms the topmost horizon of Unit II, has an inland origin. Since the borehole site is placed within the intertidal zone of a marine lagoon, this material could have been deposited by a flood event that would have transported the weathering products of the Lower Lias volcano-sedimentary formation to the coastal zone (Manupella et al., 1987). However, an alternative explanation for this terrestrial material is the tsunami produced by the 1755 Lisbon earthquake (Andrade, 1992), as this clastic sediment overlies material that has been dated at 358 cal yr BP, which is earlier than the date for the tsunami.

5. Discussion: impacts and chronology of infilling of estuarine paleovalleys during postglacial sea level rise

The sedimentary stratigraphic record may be regarded as a stack of sediment increments separated by hiatus surfaces, which occur at all levels of resolution. In other words, according to Sadler (1999), the rate of accumulation is a property of both the depositional system and the time-scale. Translated to the conditions of the progressively drowned paleovalley, a time continuous sedimentary record may be accommodated in a period of spatially constant separation of the water surface and sediment boundary. The projection of depths within the sedimentary column which are inferred to be the sedimentation surfaces against the age of dated items (Table 1) pertaining to those surfaces was plotted for the studied boreholes in Fig. 6. This graph complements a similar plot based also on borehole data, which was first proposed for the Guadiana Estuary by Boski et al. (2002). According to that work, the period of fast sediment accumulation which was covered by ^{14}C datings lasted ca 3700 years, i.e. from 10 700 to 7000 cal yr BP and corresponded to 8.5 mm yr^{-1} of vertical sediment accretion. This figure is in a fairly good agreement with the 7.6 mm yr^{-1} value proposed in the present work (Fig. 6) for a more extended period of time, starting at 13 000 cal yr BP and lasting until 7500 cal yr BP. The integration of the data from both studies gives the value of 0.66 mm yr^{-1} with the squared correlation coefficient $R^2 = 0.55$. In a recent study carried out in the Mira River Estuary on the Western Portuguese coast, Alday et al. (2006) proposed a date of 6000 cal yr BP for the beginning of deceleration in the rate of sea level rise. However, the latter figure is based on only five dated samples of sediment organic matter, of which only one is more recent than 7000 cal yr BP and, therefore, the estimate may be to low.

Considering the limited compressibility of the studied sedimentary column (Santos and Boski, 2000) due to the lack of peat layers and generally low content of organic carbon averaging 1.4% (Gonzalez Vila et al., 2003), the figure of 7 mm yr^{-1} may be proposed as the rate of sea level rise in the western part of the Gulf of Cadiz. This rate is almost one order of magnitude higher than in the following period described below. Such an accelerated pace of sediment accumulation, which may be extrapolated to the global scale, implies also a proportional increase in burial of the organic matter exported from continent to the ocean. As a consequence, during the period of rapid sea level rise, the coastal ocean receives proportionally fewer nutrients, leading to a decrease in marine primary productivity, a lower output of the marine ''biological pump'', and an increase in CO_2 atmospheric levels (Boski et al., 2006).

The remaining 9.5 m of sediments were accumulated in both estuaries in the period between 7500 cal yr BP and the present. The latter figure is obtained from the interception between the regression lines plotted for lower and upper segments of four sedimentary profiles as shown in Fig. 6. The plot of the upper segment indicates an average sediment accretion rate of 0.9 mm yr^{-1}, a value which is close to the 1.12 mm yr^{-1} reported by Perez-Arlucea et al. (2005) in the Ria de Vigo for the period 2001 to 484 yr BP, but much lower than the 1.5 mm yr^{-1} which is the present rate of sea level rise proposed by Dias and Taborda (1992). However, the depth–age relation for this period varies considerably from place to place reflecting the discontinuity of local sedimentary records, provoked by non-deposition and/or erosion, particularly evident within estuarine sand bars. The decrease of the intertidal area within the estuaries of Algarve occurred during the terminal phases of alluviation during the Late Holocene. Chester and James (1991) and Allen (2003) attribute this process to anthropogenic causes, i.e. forest cutting and agriculture which are documented throughout seven millennia of prehistoric, Roman, Moorish and Portuguese occupation.

6. Conclusions

The sediment profiles obtained from the drilling of four boreholes into the Quaternary infill of Beliche–Guadiana and Gilão–Almargem estuaries permit assessment of the processes of sedimentation during the postglacial sea level rise since ca 13 000 cal yr BP. The more sheltered sites (boreholes CM5 and G2) offer an almost continuous record of sediment accumulation in an environment of tidal flat or salt marsh as indicated by the Foraminiferal Index of Marine Influence (FIMI). Nevertheless, this paleo-ecological proxy requires further refinements through studies of the modern environment and must be interpreted in the context of complex diagenetic processes driven by the anaerobic respiration of organic matter and by underground water circulation. The sediment profiles from boreholes G1 and G3 in the Gilão–Almargem estuarine area provide information about the more discontinuous process of sedimentation in estuarine bars, controlled by the influx of sandy sediments transported by the longshore current since ca 8000 cal yr BP. All the data combined provide the curve of sediment accumulation from ca 13 000 cal yr BP to the present.

Between 13 000 and 7000 cal yr BP the level of the sediment surface rose at a rate of 7.6 mm yr^{-1}. Since then the process slowed down to ca 0.9 mm yr^{-1} and was characterized by local discontinuities. The extrapolation of these trends observed in estuarine areas on a global scale should be integrated into the global carbon cycle over the Quaternary glacial–interglacial cycles. This exercise could potentially provide an explanation for the varying atmospheric CO_2 levels observed during the Late Quaternary.

Acknowledgments

This research was financed within the framework of project FORMOSE – Sources and Retention of Organic Matter in the Estuarine Zones, PRAXIS XXI program of Portuguese Science and Technology Foundation and project MEGASIG, INTERREG IIIa program of the European Union. It is a contribution of CIMA team to UNESCO IGCP 495 project.

We thank Cari Zazo and an anonymous reviewer for their careful revision of the manuscript. Duarte Nuno Ramos Duarte is gratefully acknowledged for his help in field data processing.

References

Alday, M., Cearreta, A., Cachao, M., Freitas, M.C., Andrade, C., Gama, C., 2006. Micropalaeontological record of Holocene estuarine and marine stages in the Corgo do Porto rivulet Mira River, SW Portugal. Estuarine, Coastal and Shelf Science 66, 532–543.

Allen, H.D., 2003. A transient coastal wetland: from estuarine to supratidal conditions in less than 2000 years – Boca do Rio, Algarve, Portugal. Land Degradation and Development 14, 265–283.

Allen, J.R.L., 2000. Morphodynamics of Holocene salt marshes: a review sketch from the Atlantic and Southern North Sea coasts of Europe. Quaternary Science Review 19, 1155–1231.

Andrade, C., 1992. Tsunami generated forms in the Algarve barrier islands (south Portugal). Science of Tsunami Hazards 10, 21–34.

Andrade, C., Freitas, M.C., Moreno, J., Craveiro, S.C., 2004. Stratigraphical evidence of Late Holocene barrier breaching and extreme storms in lagoonal sediments of Ria Formosa, Algarve, Portugal. Marine Geology 210, 339–362.

Bao, R., Freitas, M.C., Andrade, C., 1999. Separating eustatic from local effects: a Late Holocene record of coastal change in Albufeira Lagoon, Portugal. The Holocene 9, 341–352.

Berrocal-Rangel, L., 2001. Los pueblos célticos del Suroeste peninsular. In: Almagro-Gorbea, M., Mariné, M., Álvares-Sanchís, J. (Eds.), Celtas y Vettones. Diputación General de Ávila, Ávila, Spain, pp. 326–333.

Bettencourt, P., 1994. Les environments sédimentaires de la côte sotavento (Algarve-Sud Portugal) et leur évolution Holocêne et actuelle. Unpublished PhD dissertation, Univ. Bordaux I, France.

Borrego, J., Morales, J.A., Pendon, J.G., 1995. Holocene estuarine facies along the mesotidal coast of Huelva, southwestern Spain. International Association of Sedimentologists, Special Publication 24, 151–170.

Boski, T., Moura, D., Camacho, S., Duarte, R.D.N., Scott, D.B., Veiga-Pires, C., Pedro, P., Santana, P., 2002. Postglacial sea level rise and sedimentary response in the Guadiana Estuary, Portugal/Spain border. Sedimentary Geology 150, 103–121.

Boski, T., Moura, D., Santos, Correia, V., Camacho, C., Veiga-Pires, C., Martins, H., Wilamowski, A., 2006. Postglacial organic carbon accumulation in coastal zones – a possible cause for varying atmospheric CO_2 levels. Journal of Coastal Research 39, 1863–1867.

Camacho, S., 2006. Holocenic evolution of Guadiana River Estuary (South of Portugal) based on benthic foraminifera assemblages. In: Proceedings of the Meeting and Abstracts of the International Symposium on Foraminifera, Natal, Brazil. Anuário do Instituto de Geociências UFRJ 29-1, pp. 410–411.

Carling, P.A., Radecki-Pawlik, A., Williams, J.J., Rumble, B., Meshkova, L., Bell, P., Breakspear, R., 2006. The morphodynamics and internal structure of intertidal fine-gravel dunes: Hills Flats, Severn Estuary, UK. Sedimentary Geology 183, 159–179.

Chester, D.K., James, P.A., 1991. Holocene alluviation in the Algarve, southern Portugal: the case for an anthropogenic cause. Journal of Archaeological Science 18, 73–87.

Choi, K.S., Khim, B.K., Woo, K.S., 2003. Spherulitic siderites in the Holocene coastal deposits of Korea eastern Yellow Sea: elemental and isotopic composition and depositional environment. Marine Geology 202, 17–31.

Choi, K.S., Park, Y.A., 2000. Late Pleistocene silty tidal rhythmites in the macrotidal flat between Youngjong and Yongyou Islands, west coast of Korea. Marine Geology 167, 231–241.

Dabrio, C.J., Zazo, C., Goy, J.L., Sierro, J.F., Borja, Lario, J., Gonzalez, J.A., Flores, J.A., 2000. Depositional history of estuarine infill during the last postglacial transgression (Gulf of Cadiz, Southern Spain). Marine Geology 162, 381–404.

Darlymple, R.W., Zaitlin, B.A., Boyd, R., 1992. Estuarine facies models: conceptual basis and stratigraphic implications. Journal of Sedimentary Petrology 62, 1130–1146.

Dias, J., Taborda, R., 1992. Tidal gauge data in deducing secular trends of relative sea-level and crustal movements in Portugal. Journal of Coastal Research 8, 655–659.

Donnici, S., Serandrei-Barbero, R., 2002. The benthic foraminiferal communities of the northern Adriatic continental shelf. Marine Micropaleontology 44, 93–123.

Edwards, R.J., Horton, B.P., 2000. Reconstructing relative sea-level change using UK salt-marsh foraminifera. Marine Geology 169, 41–56.

Fatela, F., Taborda, R., 2002. Confidence limits of species proportions in microfossil assemblage. Marine Micropaleontology 45, 169–174.

Field, J.G., Clark, K.R., Warwick, R.M., 1982. A practical strategy for analysing multispecies distribution patterns. Marine Ecology Progress Series 8, 37–52.

Fitzpatrick, R.W., Hudnall, W.H., Self, P.G., Naidu, R., 1993. Origin and properties of inland and tidal saline acid sulphate soils in South Australia. In: Dent, D.L., van Mensvoort, M.E.F. (Eds.), Selected Papers of the Ho Chi Minh City Symposium on Acid Sulphate Soils. International Institute of Land Reclamation and Development Publication 3, pp. 71–80.

Fletcher, W.J., Boski, T., Moura, D., 2007. Palynological evidence for environmental and climatic changes in the lower Guadiana valley (Portugal) during the last 13,000 years. The Holocene 17, 479–492.

García-García, A., García-Gil, S., Vilas, F., 2005. Quaternary evolution of the Ría de Vigo, Spain. Marine Geology 220, 153–179.

Gonzalez, R., Dias, J.A., Lobo, F., Mendes, I., Plaza, F., 2004. Sedimentological and paleoenvironmental characterisation of transgressive sediments on the Guadiana Shelf Northern Gulf of Cadiz, SW Iberia. Quaternary International 120, 133–144.

Gonzalez Vila, F.J., Polvillo, O., Boski, T., Moura, M.D., Andrés, J.R., 2003. A biomarker approach to the organic matter deposited in coastal estuarine sediments during Holocene: a case study in the Guadiana River estuary. Organic Geochemistry 34, 1601–1613.

Granja, H., Froidefond, J., Pera, T., 1984. Processus d'évolution morphosedimentaire de la Ria Formosa (Portugal). Bulletin de l'Institut de Géologie du Bassin d'Aquitaine 36, 37–50.

Gulliksen, S., Birks, H.H., Possnert, G., Mangerud, J., 1998. A calendar age estimate of the Younger Dryas–Holocene boundary at Krakenes, western Norway. The Holocene 8, 249–259.

Haslett, S.K., Strawbridge, F., Martin, N.A., Davies, F.C., 2001. Vertical salt-marsh accretion and its relationship to sea level in the Severn Estuary, U.K.: an investigation using foraminifera as tidal indicators. Estuarine, Coastal and Shelf Science 52, 143–153.

Hori, K., Saito, Y., Zhao, Q., Cheng, X., Wang, P., Sato, Y., Li, C., 2001. Sedimentary facies of the tide-dominated paleo Changjiang Yangtze estuary during the last transgression. Marine Geology 177, 331–351.

Hossner, L.R., Doolittle, J.J., 2003. Iron sulphide oxidation as influenced by calcium carbonate application. Journal of Environmental Quality 32, 773–780.

Lario, J., Zazo, C., Goy, J.L., Dabrio, C.J., Borja, F., Silva, P.G., Sierro, F., Gonzalez, A., Soler, V., Yll, E., 2002. Changes in sedimentation trends in SW Iberia Holocene estuaries Spain. Quaternary International 93–94, 171–176.

Manupella, G., Ramalho, M., Antunes, M.T., Pais, J., 1987. Carta Geológica de Portugal. Notícia Explicativa da Folha 53-B – Tavira. Serviços Geológicos de Portugal, Lisboa, 49 pp.

Mata, M.P., Taberner, C., Julia, R., Teagle, D.A.H., Rejas, M., de Gibert, J.M., Alfonso, P., Outeiral, P., Diaz del Rio, V., Somoza, L., 2005. Microbial mediated carbonates in the Gulf of Cádiz: data of Ibérico, Hespérides, Cornide and Fila de Hormiga. Geophysical Research Abstracts 7, 04528.

Mendes, I., Gonzalez, R., Dias, J.M.A., Lobo, F., Martins, V., 2003. Factors influencing recent benthic foraminifera distribution on the Guadiana shelf (Southwestern Iberia). Marine Micropaleontology 51, 171–192.

Morhange, C., Goiran, J.P., Bourcier, M., Carbonel, P., Le Campion, Rouchy, J.-M., Yon, M., 2000. Recent Holocene paleo-environmental evolution and coastline changes of Kition, Larnaca, Cyprus, Mediterranean Sea. Marine Geology 170, 205–230.

Moura, D., Boski, T., 1999. Unidades litostratigráficas do Pliocénico e Plistocénico no Algarve. Comunicações do Instituto Geológico e Mineiro 86, 85–106.

Nanson, G.C., Jones, B.G., Price, D.M., Pietsch, T.J., 2005. Rivers turned to rock: Late Quaternary alluvial induration influencing the behaviour and morphology of a branching river in the Australian monsoon tropics. Geomorphology 70, 398–420.

Pe-Piper, G., Dolansky, L., Piper, D.J.W., 2005. Sedimentary environment and diagenesis of the Lower Cretaceous Chaswood Formation, southeastern Canada: the origin of kaolin-rich mudstones. Sedimentary Geology 178, 75–97.

Perez-Arlucea, M., Mendez, G., Clemente, F., Nombela, M., Rubio, B., Filgueira, M., 2005. Hydrology, sediment yield, erosion and sedimentation rates in the estuarine environment of the Ria de Vigo, Galicia, Spain. Journal of Marine Systems 54, 209–226.

Pilkey, O., Neal, W., Monteiro, H., Dias, J., 1989. Algarve barrier islands: a non-coastal plain system in Portugal. Journal of Coastal Research 5, 239–261.

Ptacek, C.J., Bowles, D.W., 1994. Influence of siderite on the pore-water chemistry of inactive mine-tailings impoundments. In: Alpers, C.N., Blowes, D.W. (Eds.), Environmental Geochemistry of Sulphide Oxidation. American Chemical Society Symposium Series 550, pp. 172–180.

Redois, F., Debenay, J.-P., 1996. Influence du confinement sur la répartition des foraminiferes benthiques: exemple de l'estran d'une ria mésotidale de Bretagne. Méridionale. Revue de Paléobiologie 15, 243–260.

Rey, D., Mohamed, K.J., Bernabeu, A., Rubio, B., Vilas, F., 2005. Early diagenesis of magnetic minerals in marine transitional environments: geochemical signatures of hydrodynamic forcing. Marine Geology 215, 215–236.

Rocha, J.S., Correia, F.N., 1994. Defence from floods and floodplain management in middle size catchments. In: Gardiner, J., Starosolszky, O., Yevjevich, V. (Eds.), Defence from Floods and Floodplain Management. NATO ASI Series, Series E: Applied Sciences, vol. 299. Kluwer Academic Publishers, Dordrecht, The Netherlands, pp. 395–417.

Rodrígues, A., Magalhaes, F., Alveirinho Dias, J., 1991. Evolution of the North Portuguese Coast in the last 18 000 years. Quaternary International 9, 67–74.

Sadler, P.M., 1999. The influence of hiatuses on sediment accumulation rates. GeoResearch Forum, 15–40.

Santos, A., Boski, T., 2000. The comparison of Holocene sedimentary infill in the two areas of contrasted sedimentary dynamic of Guadiana Estuary. In: Carvalho, S.G., Gomes, V.M. (Eds.), Os Estuários de Portugal e os Planos de Bacia Hidrográfica. Associação Eurocoast, Lisbon, pp. 53–64.

Scott, D.B., Hermelin, J.O.R., 1993. A device for precision splitting of micropaleontological samples in liquid suspension. Journal of Paleontology 67, 151–154.

Studencka, B., Boski, T., Santos., A., 2003. New data on the bivalve assemblages from the Upper Miocene Deposits (Cacela Formation) of South Portugal: their environments and age. In: The Atlantic Neogene in the XXIth Century: State of the Art, Third R.C.A.N.S Congress, Tetuan, pp. 142–143.

Thorez, J., 1976. Practical Identification of Clay Minerals. Ed. Lelotte, Dison, Belgique, 87 pp.